Supporting Information

Recyclable Multifunctional Magnetic Fe_3O_4@SiO_2@Au Core/Shell Nanoparticles for SERS Detection of Hg (II)

Chao Liu [1], Hui Wang [2], Shengmin Xu [1], Hongbao Li [3], Yilin Lu [1,*] and Chuhong Zhu [4,*]

[1] Information Materials and Intelligent Sensing Laboratory of Anhui Province, Institute of Physical Science and Information Technology, Anhui University, Hefei 230601, China; chaoliuahu@163.com (C.L.)
[2] School of Chemical and Environmental Engineering, Anhui Polytechnic University, Wuhu 241000, China
[3] Institutes of Physical Science and Information Technology, Key Laboratory of Structure and Functional Regulation of Hybrid Materials, Ministry of Education, Anhui Graphene Engineering Laboratory, Anhui University, Hefei 230601, China
[4] School of Materials Science and Engineering, Anhui University, Hefei 230601, China
* Correspondence: yilin.lu@ahu.edu.cn (Y.L.); chzhu@ahu.edu.cn (C.Z.)

The Supporting Information includes:

Table S1. Comparison between this work and other reported results for detection of mercury ion.

Methods	LOD	Feature	Ref.
AAS	0.6 ng/g	High cost	[1]
AES	0.22 μg/L	Time-consuming	[2]
SERS	1 μg/L	Fast and easy	This work
ICP-MS	0.024 μg/L	Expensive equipment	[3]
AFS	4.5 ng/L	Complex operation	[4]

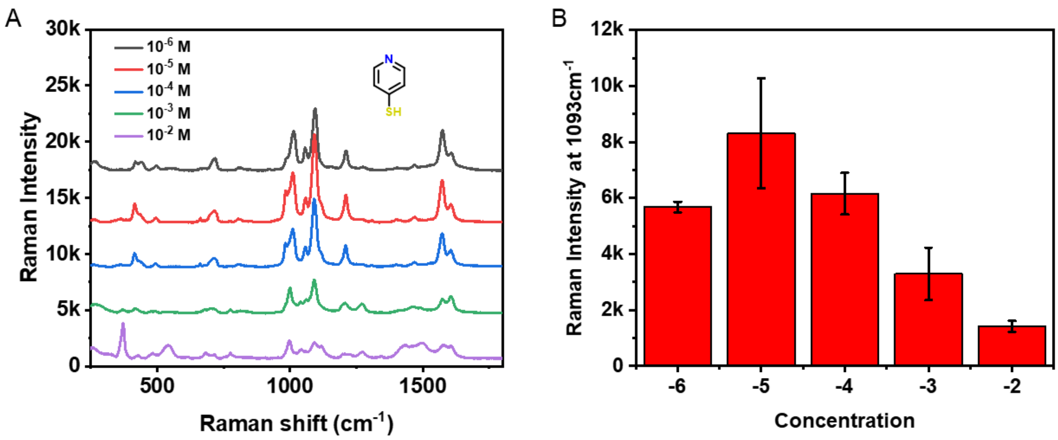

Figure S1. (A) The Raman spectra of different concentrations of 4-MPy modified on magnetic microspheres.

As shown in Figure S1, when the concentration of 4-MPy is 10^{-5} M, the SERS single of the 4-MPy is the best. So, the 10^{-5} M of 4-MPy is used as the reporter for the modification of the Au surface. The inset is structural formula of 4-MPy molecule.

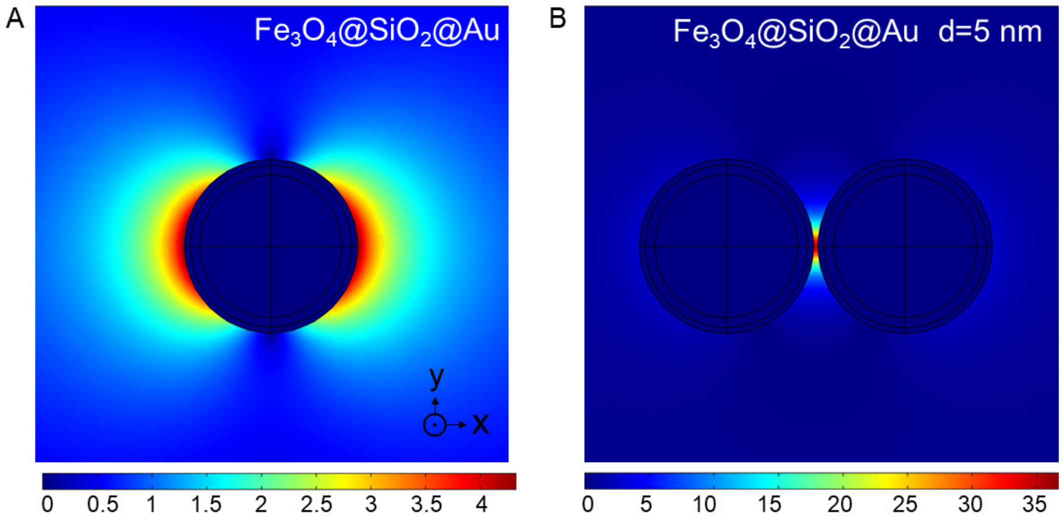

Figure S2. Electric field intensity distribution profiles using finite-element method (FEM) modeling at the excitation laser wavelength of 785 nm for (A) single MNP and (B) two $Fe_3O_4@SiO_2@Au$ MNPs with a distance of 5 nm.

FEM modeling was conducted by adopting the RF module of Comsol Multiphysics V3.5a, parameters were based on those of the core/shell nanoparticles from SEM observations such as the central distance between all the adjacent NRs (100 nm), the diameters of the NRs (45-95 nm), the length of the NRs (~200 nm), and together with the excitation line of 785 nm. Optical constants of Au and dielectric constants of SiO_2 and Fe_3O_4 were adopted from the literature [5][6].

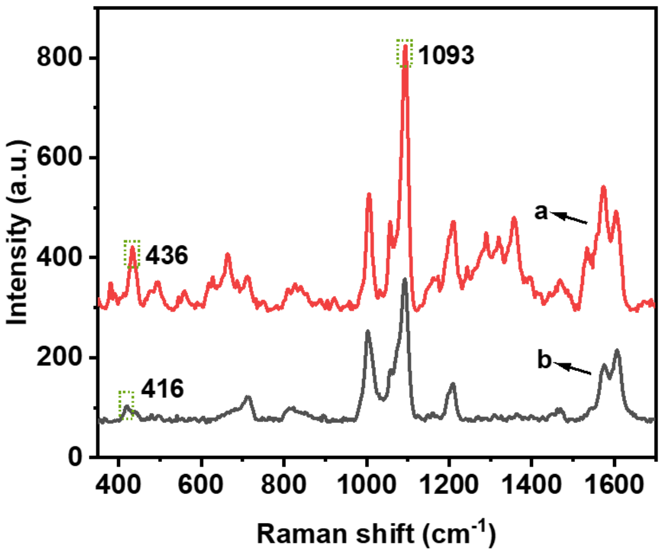

Figure S3. Raman signal of MNPs sensor in cell under 785 cm^{-1} lasers. (a) Signal of MNPs in cells after incubated with Hg^{2+}. (b) Signal of MNPs in cells. Compared with the Raman signal in water, and the Raman signal in the cell fluctuates slightly. However, it still can clearly see the signal enhancement at 1093 cm^{-1} and the peak shift at 416$cm^{-1}$and 436cm^{-1}.

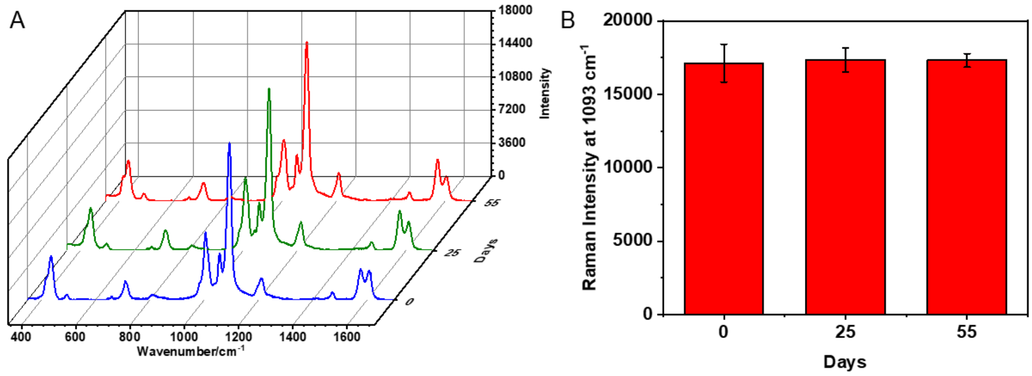

Figure S4. (A) The Raman spectra of MNPs sensor with Hg^{2+} for different days; (B) the Raman intensity of the sensor at 1093 cm^{-1} recorded within different storage time.

For Raman sensors, stability is particularly important. Figure S4A,B are the overall spectrum of the sensor within 55 days and the peak intensity at 1093 cm^{-1}, respectively. It can be seen that the sensor remains stable within 55 days.

Reference

1. Panichev, N.A.; Panicheva, S.E. Determination of total mercury in fish and sea products by direct thermal decomposition atomic absorption spectrometry. *Food Chem.* **2015**, *166*, 432–441. https://doi.org/10.1016/j.foodchem.2014.06.032.
2. Savoie, J.; St-Louis, R.; Clément, M. Facilitating local analysis in northern regions: microwave plasma-atomic emission spectrometry for mercury determination in wild Atlantic salmon. *Int. J. Environ. Anal. Chem.* **2018**, *98*, 582–591. https://doi.org/10.1080/03067319.2018.1483499.
3. Li, Y.; Chen, C.; Li, B.; Sun, J.; Wang, J.; Gao, Y.; Zhao, Y.; Chai, Z. Elimination efficiency of different reagents for the memory effect of mercury using ICP-MS. *J. Anal. At. Spectrom.* **2006**, *21*, 94–96. https://doi.org/10.1039/b511367a.
4. Li, Y.; Zhu, Z.; Zheng, H.; Jin, L.; Hu, S. Significant signal enhancement of dielectric barrier discharge plasma induced vapor generation by using non-ionic surfactants for determination of mercury and cadmium by atomic fluorescence spectrometry. *J. Anal. At. Spectrom.* **2016**, *31*, 383–389. https://doi.org/10.1039/C5JA00300H.
5. Huang, Z.; Meng, G.; Huang, Q.; Chen, B; Zhu, C; Zhang, Z. Large-area Ag nanorod array substrates for SERS: AAO template-assisted fabrication, functionalization, and application in detection PCBs. *J. Raman Spectrosc.* **2013**, *44*, 240–246. https://doi.org/10.1002/jrs.4184.
6. Ordal, M.A.; Long, L.L.; Bell, R.J.; Bell, S.E.; Bell, R.R.; Alexander Jr., R.W.; Ward, C.A. Optical properties of the metals Al, Co, Cu, Au, Fe, Pb, Ni, Pd, Pt, Ag, Ti, and W in the infrared and far infrared. *Appl. Opt.* **1983**, *22*, 1099–1119. https://doi.org/10.1364/AO.22.001099.